

# Interior Acoustic Simulation for In-Car Audio Design

Soonkwon Paik, Hyundai Motor Co., Seoul, Korea

Manu De Geest and Koen Vansant, LMS International, Leuven, Belgium

Today's automotive audio components have to meet high quality expectations with ever-decreasing development costs. Predictive methods for the performance of sound systems in view of the optimal locations of loudspeakers in a car can help to overcome this challenge. This article describes a number of sound-field simulation tools to model the acoustic and vibro-acoustic aspects that come into play when transducers are mounted into small areas such as passenger compartment and door cavities. Examples are shown how FEM software can predict the acoustic modes of passenger compartments and door cavities. Automatic volume meshers are key to the success of the Acoustic FEM solutions. Vibro-acoustic effects, such as speaker membrane vibrations coupled with door cavity acoustic pressures and vibrations on the door trim can be taken into account using coupled structural and acoustic FEM and BEM formulations. Also fast-multipole BEM is used to boost the realistic frequency range up to 5000 Hz and higher. For very-high-frequency modeling (above 5000 Hz), beam-tracing algorithms based on principles of ray acoustics can be deployed to synthesize binaural impulse responses and deriving IACC-index maps. Aspects of absorbent material properties (complex acoustic impedance) and speaker characterization (velocities) are discussed.

Driven by customers who spend a lot of time in their cars, automakers challenge their infotainment departments and audio suppliers with an ever-increasing demand on abundant audio and multimedia applications inside vehicles, such as high-fidelity surround systems, Bluetooth phone communication, audio-assisted navigation systems, or voice-operated control systems.

How does one design and optimize all passive and active components that influence in-vehicle acoustic comfort? And how to do this in compressed development time, preferable early in the vehicle development cycle, so not to compromise quality and cost?

This article discusses some of the predictive methods that aim to reduce development time and increase in-vehicle audio sound quality by means of sound-field simulation software.<sup>2</sup>

## Acoustic and Vibro-Acoustic Parameters

**Sound Fields in Small Rooms.** Automotive passenger compartments can be considered very small rooms in terms of their acoustical properties. Depending on the frequency, the acoustics inside the car exhibit very different physical behaviors. At low frequencies, wave acoustics dominate with a limited amount of widely separated acoustic modes. At high frequencies, the sound field becomes more and more diffuse, making it more convenient to describe the sound field statistically. In this region peaks and dips do not correspond to eigen frequencies of acoustic modes but are the result of numerous overlapping resonances. The term *spectral coloration* is used to characterize this phenomenon. Often the Schroeder cut-off frequency is suggested to mark the transition between low- and high-frequency regions. This is about 300 Hz in a typical car compartment.

**Cabin Modes.** The low-frequency performance of a vehicle audio system is closely related to the cabin modes, which are considered useful to support the low-frequency auditory experience. For this reason it is of paramount importance that the woofer loudspeakers are placed so that they can couple with these modes. These

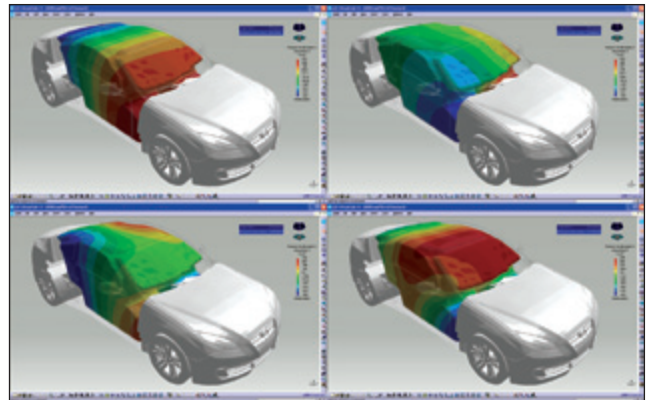


Figure 1. First longitudinal and lateral modes of a Hyundai Genesis coupe at 64, 73, 108 and 115 Hz.

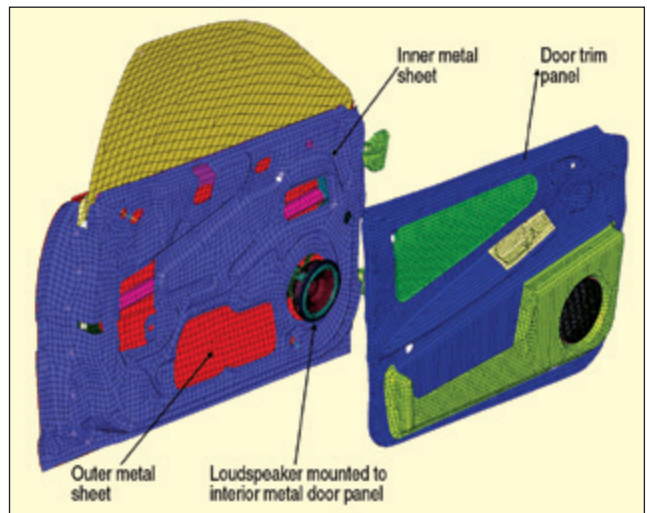


Figure 2. Structural model for the front left door of a passenger car.

locations are often in the front or rear corners of the interior. See Figure 1 for the first longitudinal modes of a coupe. Obviously the eigen frequency values of these mode shapes depend very much on the type of the vehicle – sedan, SUV, monospace, coupe, etc.

**Automotive Doors.** Next to the acoustic behavior of the vehicle cavity, the audio system performance is also influenced heavily by the acoustics of the doors. Indeed, an important part of loudspeaker design in audio applications concerns cabinet design. Influences of cabinet size, shape and flexibility will show up in the resulting radiated sound pressure field, which will deviate from the response of an idealized “diaphragm in an infinite rigid baffle” loudspeaker. For automotive applications, the cabinet consists of metal inner and outer door panels and the trim panel. Figure 2 illustrates the door assembly. Some geometric parameters of the door are fixed – trim and outer metal panel shapes as well as the total door volume are inherent to pure stylistic and ergonomic car design parameters.

However, there are dangers attached to mounting loudspeakers in inner door panels. If contact areas exist between the vehicle cavity and the door cavity (such as door trim gaps and watershed holes), a coupling of the modes can result in door cavity modes absorbing some of the energy that was supposed to be transferred

Based on a paper presented at Inter-Noise 2011, 40th International Congress and Expo on Noise Control Engineering, Osaka, Japan, September 2011.

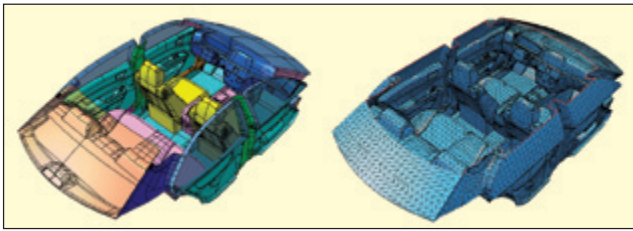


Figure 3. CATIA V5 CATPart model of Hyundai Sonata cabin interior (left) and tessellated version (right).

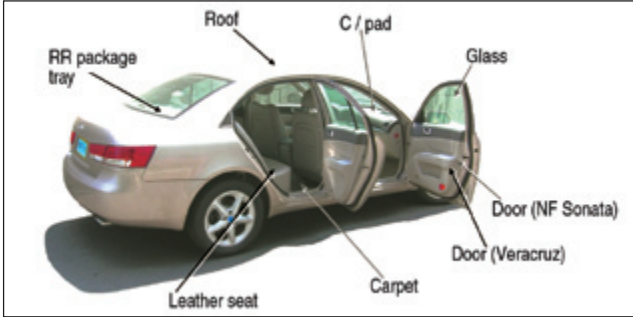


Figure 4. Material property group assignment in Hyundai Sonata.

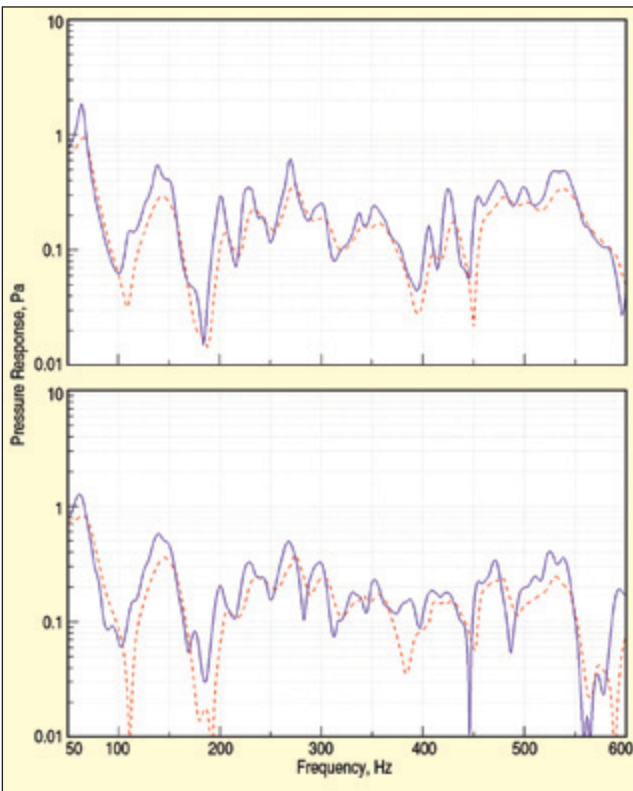


Figure 5. Influence of complex impedance applied in a box-shaped 2.5x1.5x1.2 m enclosure. Red – Real Impedance 7657 Rayl; Blue – Complex Impedance 7657 - i 7657 Rayl; Top – BEM simulation; Bottom – RAY simulation.

to the vehicle cavity.<sup>6</sup>

Other problems of vibro-acoustic nature can arise with the door trim. For fuel economy reasons, the door weight is often minimized by reducing the thickness of all panels and the area of the inner metal door sheet. One can imagine this can have a possibly negative effect on loudspeaker performance. As the door panels become lighter, they will be more actively engaged in the vibro-acoustic response triggered by the loudspeaker electrical input signal.<sup>5</sup>

The resulting pressure field in the cabin will come not only from the vibrating loudspeaker diaphragm but also from the sound-radiating trim panel. The influence of the latter can contaminate the tone color. More lightweight flexible panels will also cause more

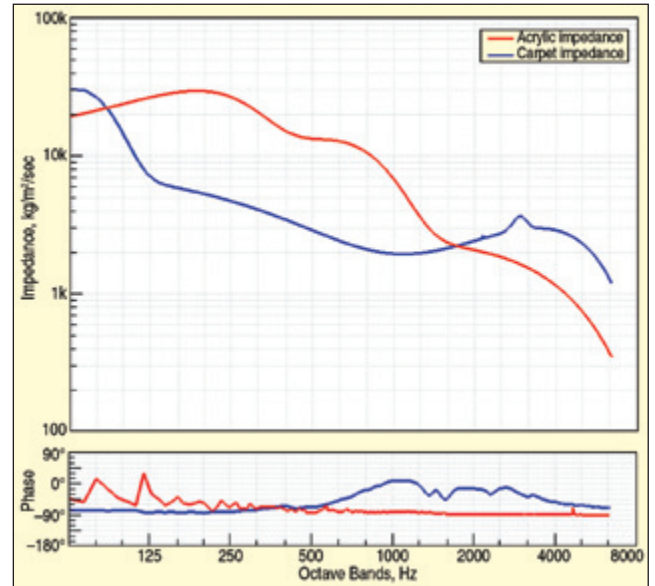


Figure 6. Measured acoustic impedances of acrylic plastic and carpet by means of Kundt's tube.

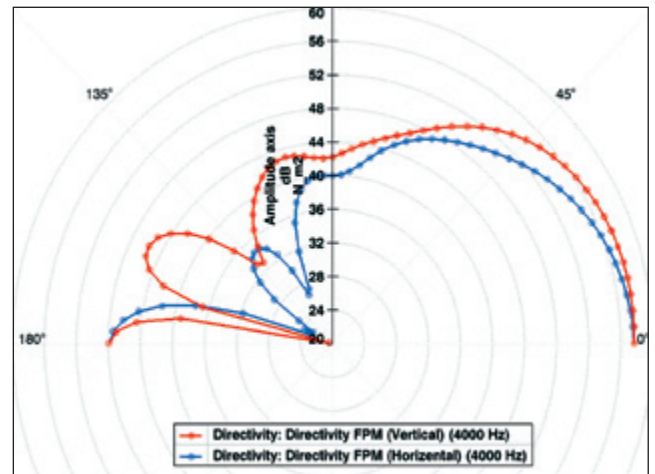


Figure 7. Polar directivity data from 0° to 180° in 3° steps, and frequency from 20 Hz to 20 KHz in LogStep 1.145.

vibration of the loudspeaker unit, which has a certain mass and is mounted onto the interior metal door panel. Some alternatives come from separate enclosures that are specially designed to fit into the door volumes and under rear package shelves.<sup>7</sup>

**Reflections.** At frequencies above 500 Hz, the sound field in vehicle interiors is dominated by complex interference effects between direct and reflected waves from surfaces, such as glass windows, dashboards, carpet floors, roofliners, leather seats, etc. Spectrally, these reflections cause sound coloration, while in the time domain, they are responsible for the subjective impression of sound image and sound stage. Some of these reflections can be beneficial for the stereo balance, while others cause an in-the-box feeling.

### In-Car Audio Design Techniques

**Cabin Geometry.** Three-dimensional simulation algorithms can only be established with the existence of 3D CAD models of the automotive interior. Auto OEMs have these typically available in CATIA V5 (.CATProduct, .CATPart), Siemens NX, Pro/Engineer or neutral file formats such as IGES (.igs) and STEP. Sometimes CAD models are made available through portals such as Google 3D Warehouse, or TurboSquid (Figure 3). These CAD data files form the basis for the idealization (i.e., surface and volume meshing and tessellation) needed by the simulation solvers.<sup>1</sup>

**Absorbent Material Properties.** The absorbent material properties of the various material linings that make up the vehicle interior (see Figure 4) are specified by complex acoustic impedances (Rayl).

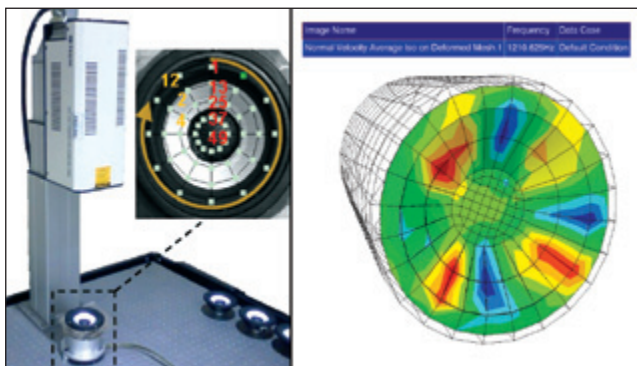


Figure 8. Measured normal velocities on a speaker membrane at 1210 Hz.

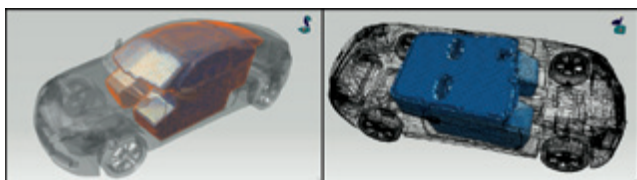


Figure 9. Automatic volume FE cavity meshing excluding seats of the Genesis coupe.

The real term of this magnitude (resistance) represents the energy losses that impinging waves undergo, while the imaginary term (reactance) represents the phase changes.<sup>4</sup> For locally reacting materials, acoustic impedances have a relationship with an angle of incident-dependent reflection coefficient. The latter is more convenient to be used in a ray-acoustic model (see subsequent section on high-frequency stimulation).

Figure 5 shows a simulated frequency response within a small volume of  $2.5 \times 1.5 \times 1.2$  m, a real impedance of 7657 Rayl, and a complex impedance of  $7657 - 7657i$  Rayl. This shows the influence of the imaginary term on the frequency response curve.

Acoustic Impedances can be measured with various techniques, of which Kundt's tube is the most known. Figure 6 shows an example of a measured, frequency-dependent complex impedance for acrylic plastic and carpet surface.

**Speaker Characterization.** A loudspeaker is typically characterized by its on-axis frequency response and its directional polar diagram (see Figure 7). A more direct way to characterize a speaker in baffled and anechoic conditions is to measure the normal velocities of its vibrating membrane by means of a laser Doppler vibrometer with an input signal such as pink noise (2V) and measuring frequency range of 0–4000 Hz (8 Hz intervals). See Figure 8.

## Low- and Mid-Frequency Simulation

**Principles.** When it comes to acoustics and virtual design simulation, there are two primary methods: the boundary element method (BEM) and the finite element method (FEM).

Acoustic harmonic FEM is used to predict acoustic responses in the frequency domain or to evaluate acoustic mode shapes of cavities. The method requires a mesh of the acoustic domain and leads to a system of equations with banded system matrices, which are solved in a very efficient manner using iterative or direct solvers. Acoustic, harmonic, finite-element models are excited through a set of sound sources in the domain or by imposed normal surface velocities at the boundary or by defined pressures at selected nodes. The velocities can be imported from vibration tests or from structural FEA codes. Acoustic damping is introduced through porous materials (volume absorbers), trim liners (surface absorbers) and fluid damping. The method yields results at all FE nodes and at any field point in the domain.

Acoustic harmonic BEM allows the user to solve acoustic radiation problems and to predict the acoustic response in both enclosures and unbounded domains. It only requires a mesh of the surface boundary fluid domain, resulting in a low number of degrees of freedom. The user specifies a frequency range and intermediate steps, with no constraints on either. Different ranges and steps can be combined. Acoustic boundary-element models can

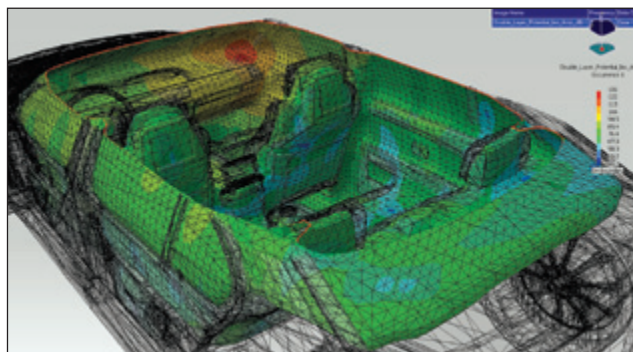


Figure 10. Frequency response at 750 Hz from right midrange speaker at instrument panel (simulation with fast-multipole BEM).

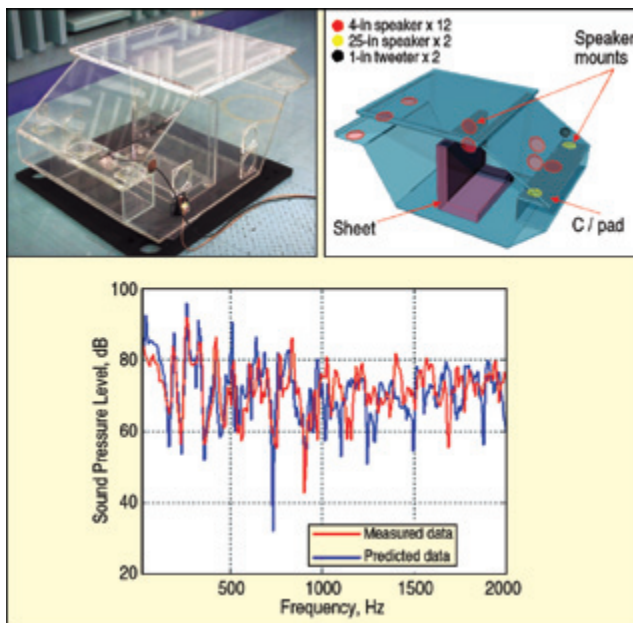


Figure 11. Validation of BEM simulation in a half-scale acrylic car interior.

be excited by a set of sound sources in the domain or by imposed normal surface velocities or surface pressures on the boundary. These boundary conditions can be imported from vibration tests, from structural FEA codes or using generic values. Acoustic damping is introduced through surface-impedance boundary conditions; the method yields results at any field point.

Virtual.Lab™ from LMS International provides tools that enable a cavity FE mesh to be generated directly from a structural model or CAD data, thereby handling sharp and smooth features, seats and footprints (see Figure 9). There is one fundamental difference between BEM and FEM. With BEM, one discretizes only the surface of the radiating body, while with FEM, the entire acoustic domain must be discretized. Because with BEM all numerical approximations are confined to the surface, a smaller mesh can be used as compared with FEM for the same accuracy.

Yet standard BEM can potentially lead to large computational times and memory requirements, it may be prohibitive to apply to very large problems. Moreover, the direct link between the frequency of analysis and the required number of elements to obtain a good enough accuracy tends to limit the use of standard BEM to the lower frequency range.

Fast-multipole BEM (FMBEM) breaks these limits by considerably accelerating the computational process and by drastically reducing the memory requirements. Thanks to this new technology, large industrial problems with one million degrees of freedom and more can be practically solved, and acoustic simulations at much higher frequencies become possible. With FMBEM applied to car interior simulation, frequency ranges up to 4000 Hz and higher are within reach. (See Figure 10).

**Validation.** In a validation study, the BEM method was applied to model the acoustics of a half-scale acrylic plastic mock-up cav-

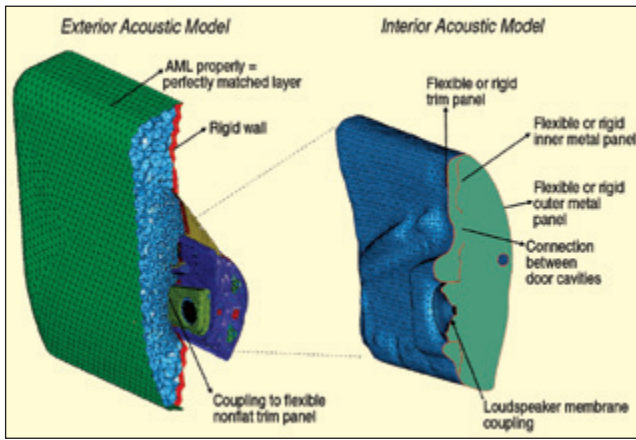


Figure 12. Vibro-acoustic model of passenger car front left door, idealized loudspeaker, infinite baffle.

ity. Various configurations were tested such as multiple speaker/microphone locations with and without seats (Figure 11).

**Vibro-Acoustic Simulation of Loudspeakers in Automotive Doors.** To look at how the parameters of an automotive door influence the loudspeaker response, several vibro-acoustic loudspeaker simulation models are discussed in this section:

- Model 1 – infinite baffle, ideal loudspeaker model.
- Model 2 – rigid car door cabinet, for assessing effects of the actual non-flat door trim panel and the effect of the fluid volume in the door cavity on the loudspeaker; all panels are modeled as being rigid.
- Model 3 – flexible trim panel plus rigid metal sheet car door cabinet, for investigating how the trim vibrations change the total radiated sound. Note that there is no connection modeled between the loudspeaker and the trim panel, as the former is mounted onto the inner metal door panel. This means the trim panel in this case is excited only acoustically.
- Model 4 – flexible door and trim panels in car door cabinet; similar to previous case but with the effect of metal panel flexibility; most realistic model including all effects. The door model is attached to the environment by weather strip sealing and by connections to hinges and a latch that are fixed to ground.

For all models, an excitation of 0.08 N force load was applied at the center of the loudspeaker membrane at all simulated frequencies. A FEM approach for both structure and fluid was used. For the structural model, a modal basis was first computed (Nastran sol 103) and the vibro-acoustic models (see Equation 1) were set up and solved using LMS Virtual.Lab™ acoustics powered by the LMS Sysnoise™ solver:

$$\begin{bmatrix} \Phi_s^T & 0 \\ 0 & I \end{bmatrix} \begin{bmatrix} K_s & K_c \\ 0 & K_a \end{bmatrix} + j\omega \begin{bmatrix} C_s & 0 \\ 0 & C_a \end{bmatrix} - \omega^2 \begin{bmatrix} M_s & 0 \\ -\rho_0 K_c^T & M_a \end{bmatrix} \begin{bmatrix} \Phi_s & 0 \\ 0 & I \end{bmatrix} \begin{bmatrix} q_i \\ p_i \end{bmatrix} = \begin{bmatrix} \Phi_s^T F_{si} \\ F_{ai} \end{bmatrix} \quad (1)$$

In Equation 1,  $\Phi_s$  represents the modal basis of the structure, which reduces the problem size from  $n_s+n_a$  degrees of freedom to  $m_s+n_a$ , with  $m_s$  being the number of structural modes.  $K_s$ ,  $K_a$ ,  $M_s$ ,  $M_a$ ,  $C_s$ , and  $C_a$  are the structural and acoustical stiffness, mass and damping matrices.  $K_c$  is the coupling matrix between the structural and acoustic model, which is responsible for the pressure loading from the fluid on the structural model and ensures continuity of structural and acoustical velocities at the interface. The unknowns are the nodal pressures  $p_i$  and modal coordinates  $q_i$ .

The solver used for these cases is a multi-frontal massively parallel sparse direct solver (MUMPS), which allows speeding up computation time by means of parallel computing. Another factor that enabled fast computations (couple of hours for the largest cases with fully coupled door) is the model size. For the models sketched in Figures 12 and 13, the interior car cabin is not taken into account. Instead, a full half-space on the inner side of the door is considered to fully concentrate on only the door vibro-acoustic phenomena. The FEM model can of course not extend to infinity to fill up the half-space. Therefore a perfectly matched layer (PML) technique is used at the FEM boundary, which guarantees

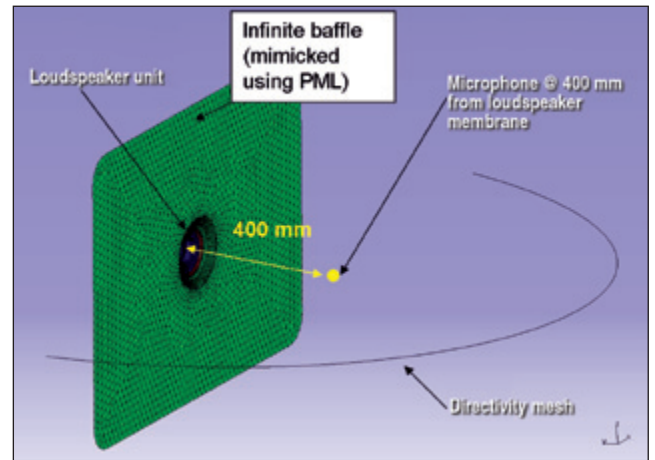


Figure 13. Vibro-acoustic model of loudspeaker unit mounted into infinite baffle.

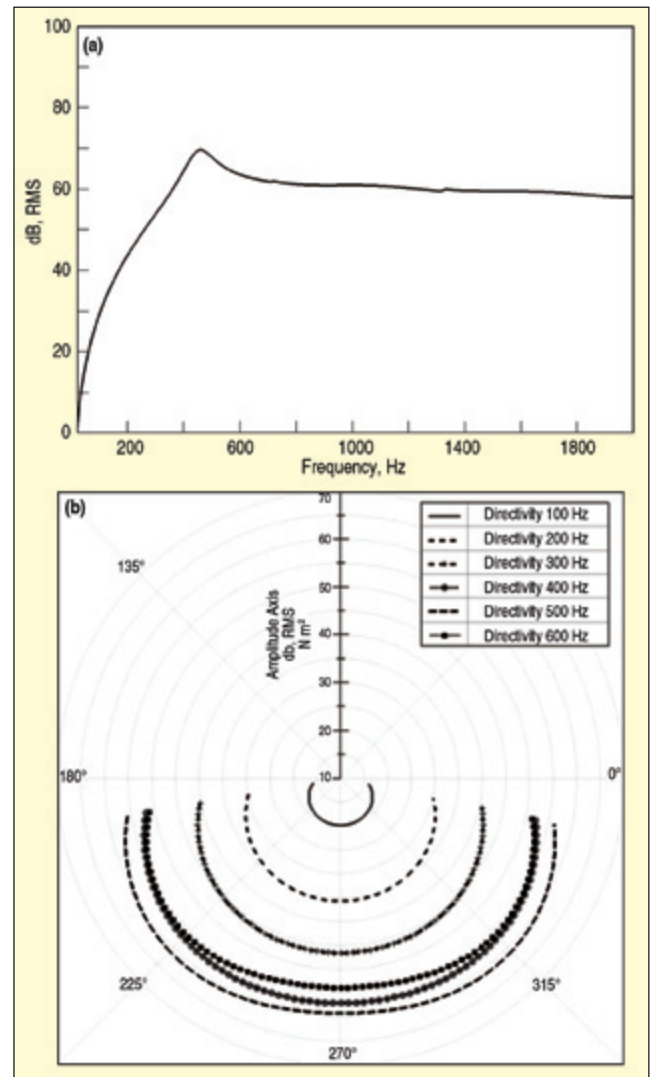


Figure 14. Top: frequency response at 400 mm from loudspeaker; bottom: directivity in 100 Hz increments, loudspeaker in rigid, infinite baffle.

an anechoic boundary of the FEM domain. More details on the PML technology can be found in Reference 10.

Two common characteristics of a loudspeaker are computed using these approaches: on axis frequency response (distance of 400 mm from membrane) and the directivity of the radiated sound toward the interior of the car.

To validate the loudspeaker model, responses were computed between 20 Hz and 2 kHz for the idealized first case, which contains a loudspeaker mounted into an infinite baffle. Figure 13 illustrates

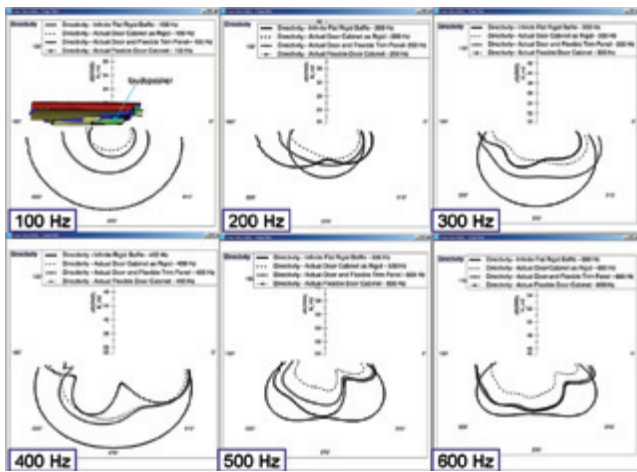


Figure 15. Directivity plots for different loudspeaker setups: infinite flat baffle; rigid car door enclosure; car door enclosure with flexible trim panel (only acoustically excited); and fully flexible car door enclosure.

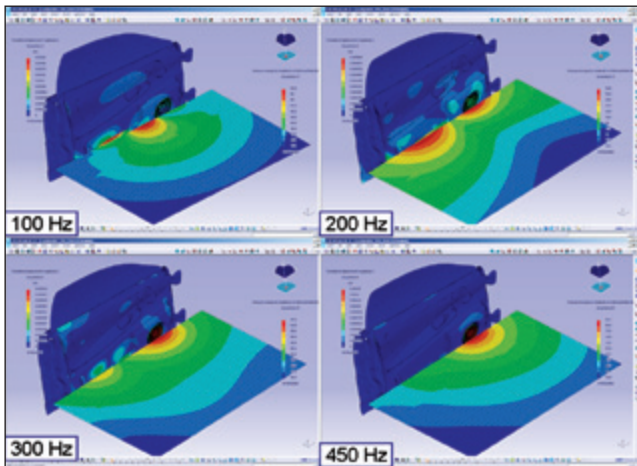


Figure 16. SPL response for flexible car door cabinet, which shows how trim panel disturbs ideal radiated pressure field in low frequencies.

the setup, while Figure 14 shows the SPL result for an on-axis microphone removed 400 mm from the loudspeaker diaphragm and the directivity of the radiated pressure field into the half space. A normal behavior can be observed; the SPL ramps up to the first resonance frequency at 462 Hz of the membrane (on-axis movement of membrane with respect to the loudspeaker basket). The directivity looks like a monopole in the lower frequencies. Comparison with the other models will go up to 600 Hz only as the car door model's accuracy cannot be guaranteed for higher frequencies.

Figure 15 reveals the directivity results for all assemblies described previously. For each plotted frequency, the isolated effects including the actual door volume, incorporating flexibility of the trim panel, and using a flexible model for the full door can be observed.

At the higher frequencies (500 and 600 Hz), the directivity pattern seems to be defined mostly by the shape of the trim panel and door cavity but not so much by its flexibility. Making the trim panel flexible or the full car door flexible doesn't seem to change the shape of the directivity but only the amplitude of the radiated sound. At these frequencies the speaker membrane vibrations are much higher compared to the vibrations on the remainder of the door (the loudspeaker assembly).

At lower frequencies, however, the directivity shape seems to be influenced more severely by the flexibility of the trim panel and the metal sheet door panels. The vibrations on the trim panel result in a rather important contribution to the total radiated pressure field that therefore deviates from the acoustic radiation of a rigidly mounted loudspeaker. A large part of the trim panel vibrations in the flexible models is caused by structural excitation; the loudspeaker is mounted onto the inner metal door panel of the flexible door assembly. The electrical signal forces a vibration of

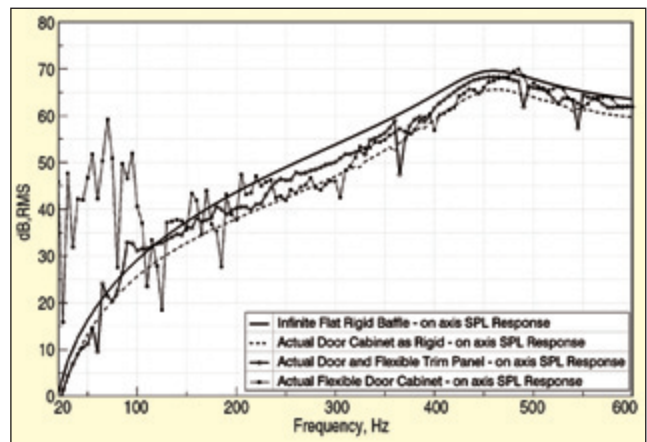


Figure 17. On-axis SPL response for different assemblies of the loudspeaker; infinite flat baffle (rigid car door cabinet); car door cabinet with flexible trim panel (only acoustically excited); and full flexible car door cabinet.

the loudspeaker membrane along the speaker's coil, but because of inertia of the loudspeaker unit and if the inner metal sheet is flexible enough, vibrations are induced in all door panels at lower frequencies (relatively far away from the first membrane resonance).

In the third model, however, only the trim panel is flexible, and it does not see a structural load from the loudspeaker, which is attached only to the Model 3 rigidly modeled inner sheet. Here the trim panel gets excited only by coupling with the air volume in the door. As can be seen in Figure 15, this acoustic coupling effect increases the amplitude of the resulting pressure field response compared to Model 2, which contains only rigid panels. For the fully flexible door, we can therefore conclude that structural compliance toward both the mounting forces of the loudspeaker unit as well as toward fluid pressure loading play a role in the total response. The effects of lower frequencies can also be seen in Figure 16. At 200 Hz, for example, one can clearly see how the trim panel has in fact two sources of sound: the loudspeaker and a locally vibrating surface.

To conclude, Figure 17 clarifies how lower frequencies modify the on-axis SPL response for the fully flexible car door case. We can expect the loudspeaker sound to be more distorted especially at these lower frequencies.

## High-Frequency Simulation

**Principles of Ray-Acoustic Models.** All numerical models derived from geometrical acoustics (GA) treat sound waves as rays following similar reflection laws as light rays in geometrical optics. The results are less accurate than the FEM or BEM methods described previously, but its validity increases substantially with higher frequencies. The LMS Virtual.LabRay-acoustics software applies a triangular beam-tracing method (TBM) to find visible image sources efficiently. The algorithm is equipped with compensation terms for physical phenomena such as constructive and destructive interference, wall diffusion or scattering, diffraction around sharp edges, echogram tail corrections, etc.

Added values of ray-based methods are legion. First, no mesh discretisation is required. As a matter of fact, one can work almost directly with CAD data after a simple tessellation process (provided with LMS Virtual.Lab). Moreover, there is no upper limit to the frequency range, and the computation runs are fairly fast. Last but not least, ray-acoustic algorithms also provide directional information which enables binaural synthesis thereby taking into account head-related transfer functions (HRTF).

**Validation.** TBM in cars can be applied typically from 5 kHz onward. Figures 18 and 19 show that the ray results can match BEM even at lower frequencies.

**Time Domain Analysis.** One of the advantages of ray-acoustic models is their ability to produce frequency results with very high resolution, so that conversion to the time domain yields detailed wave propagation animation. Figure 20 shows the result of a simulated pressure impulse response in the Hyundai Genesis coupe at the driver's head location from two tweeters mounted on

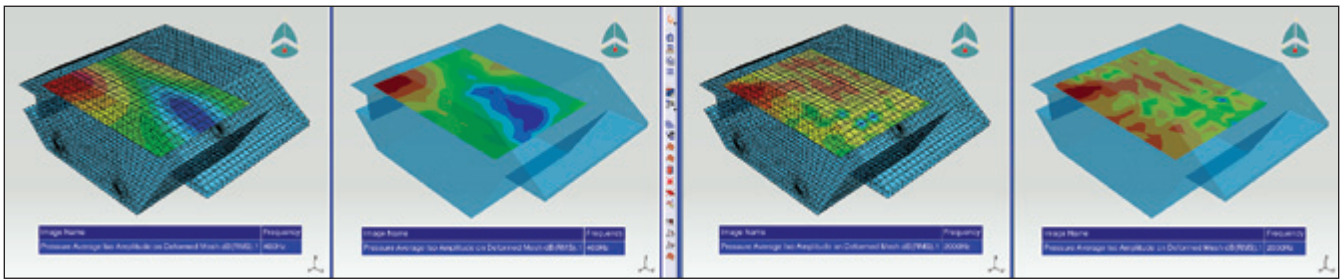


Figure 18. Validation of TBM (right) with BEM (left) reference in small car cavity at 500 Hz (left) and 2 kHz (right).

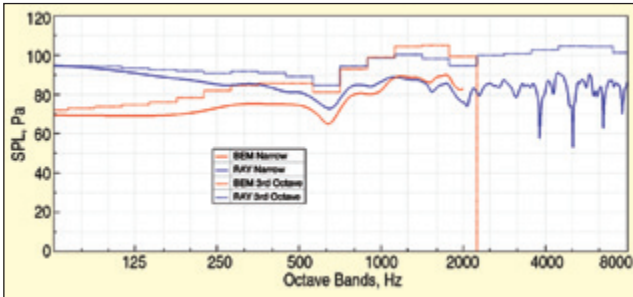


Figure 19. Comparison BEM vs. ray acoustics in geometry described in Section 3.4.2.

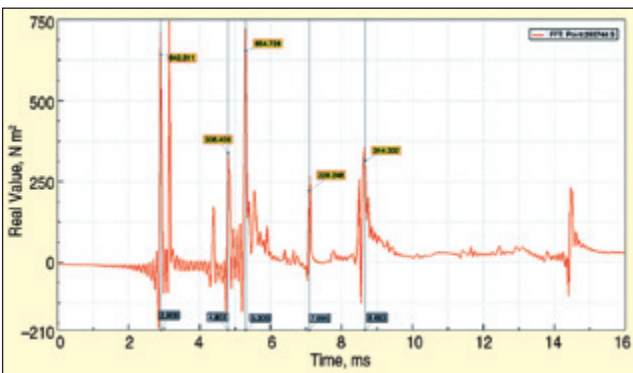


Figure 20. Simulated pressure impulse response at driver's head location from two tweeters left and right in the corner of the instrument panel.

the instrument panel.<sup>3,8</sup> Table 1 lists the number of acoustic waves arriving at the driver's head location at different arrival times.

**Binaural Synthesis.** Binaural synthesis consists of converting the echogram into a pressure impulse response stored in a FIR-filter, thereby convolving each impinging ray wavefront with its corresponding head-related impulse response based on its azimuth and elevation angle as shown in Figure 21. The angular resolution of the HRTF libraries depends on the provider. Virtual.Lab ray-acoustics supports KEMAR HRTFs provided by MIT Media Lab and HRTFs provided IRCAM. IRCAM offers many HRTF libraries for different listener subjects (each with specified morphological attributes).<sup>11,12</sup> Figure 22 shows the resulting binaural impulse response of the case described in section on time-domain analysis.

**Sound Quality Assessment.** Sound quality can be assessed by a number of objective and subjective indices. One of them is the interaural cross-correlation (IACC). IACC is a binaural measure of the difference in sound at the left and right ear. It has been demonstrated to have an objective relationship with subjective effects, such as spaciousness, apparent source width (ASW) and listener envelopment (LEV).<sup>13</sup>

Figure 23 shows the influence of a 2-ms delay and 5-dB gain in the right tweeter on the IACC map in the front row seating area. The IACC at the driver's head has increased from 0.2 to 0.5, indicating improved spatial impression.

## Conclusions

In this article, the acoustic and vibro-acoustic phenomena that are to be dealt with in a car audio design were discussed along with acoustic cabin modes, vibro-acoustic behavior of the automo-

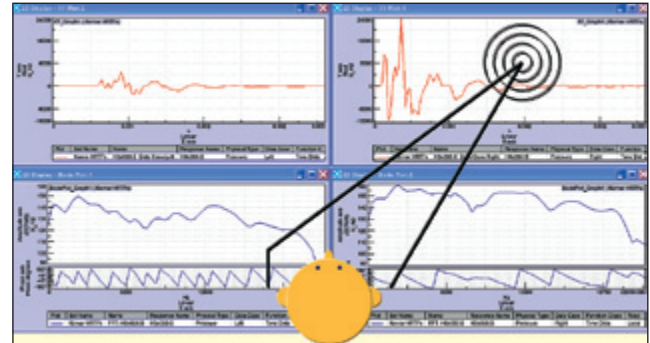


Figure 21 - Kemar HRIR/HRTF - elevation 0°, azimuth 50°.

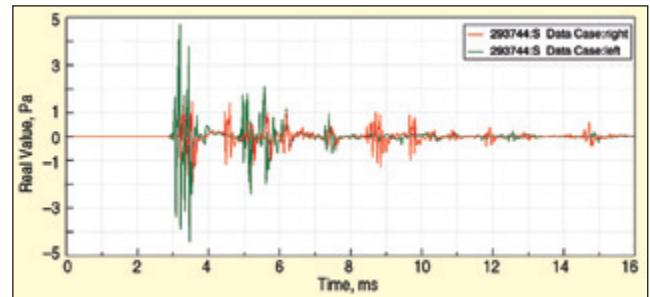


Figure 22. Binaural impulse response (BIR) at driver's head location from two tweeters at instrument panel.

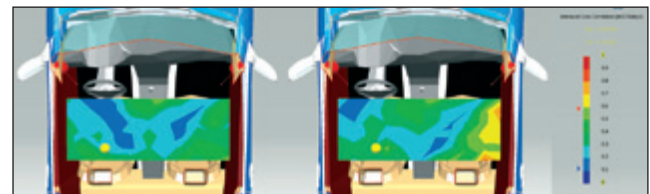


Figure 23. IACC (early)-map; symmetrical conditions (left); 2-ms delay in left tweeter and 5 dB gain in right tweeter (right).

tive door and the high-frequency reflections occurring in the car interior. As of today, there exist no single simulation technique that is capable of modeling all these effects in the full audio frequency range, so a hybrid approach should be followed. The applicability of BEM and FEM methods were shown in concrete cases, with special focus on the more recent fast-multiple BEM method and perfectly matched layer (PML) techniques. Also the ray-based methods have proven their usability.

## Acknowledgements

The authors express their gratitude to the Acoustics and Vibration Lab of Seoul National University and Advanced Automotive Research Center, as well as Hyundai Motor Company for their kind permission to publish this article.

## References

- Marc Aretz, *et al.*, "Sound Field Simulations in Car Passenger Compartment Using Combined Finite Element and Geometrical Acoustics Simulation Methods," *Proc. Aachen Acoustic Colloquium*, 2009.
- Alfred J. Svobodnik and Gabriel Ruiz, "Virtual Development of Mercedes Premium Audio Systems," AES 36th International Conference, Dearborn, MI, 2009.

Table 1. Ray paths to driver's head at different arrival times.

Arrival Time	Ray Path
2.9 ms	Direct from left tweeter
4.8ms	Direct from right tweeter
5.3ms	Right tweeter first-order reflection against windshield
7.1ms	Right tweeter first-order reflection against left window
8.3ms	Right tweeter second-order reflection against middle console and left window

3. Michael Strauss, *et al.*, "Approach to Sound Field Analysis and Simulation," AES 36th International Conference, Dearborn, MI, 2009.
4. Olivier Léost, *et al.*, "Audio Simulation of an In-Car Entertainment System," *Proc. 1999 Noise and Vibration Conference*, Society of Automotive Engineers, Inc., p. 342, 1999.
5. Mansinh Kumbhar, *et al.*, "Investigation of Factors Influencing Vehicle Audio Speaker Locations for Better Sound Quality and Spread," *Proc. SAE International*, 2007-01-2318 2007.
6. Rodrigo Nicoletta, Alice Botteon Rodrigues, "Influence of Vehicle Front Door Acoustic on Low Frequency Audio Response," *Proc. InterNoise 2005 Congress and Exposition on Noise Control Engineering*, Rio de Janeiro, Brazil, 2005.
7. Roger Shively, "Automotive Audio Design (A Tutorial)," AES 109th Convention, Los Angeles, CA, September 2000.
8. Roger Shively, *et al.*, "Optimal Location and Orientation for Midrange and High-Frequency Loudspeakers in the Instrument Panel of an Automotive Interior," AES 129th Convention, San Francisco, CA, November 2010.
9. Michael Vorländer, "Simulation and Auralization of Broadband Room Impulse Responses," *Proc. TechAcustica*, Cadiz, 2009.
10. Hadrien Beriot, Michel Tournour, "Perfectly Matched Layers for Time Harmonic Acoustics," *Numerical Methods for Acoustics Problems* (to be published).
11. IRCAM Hrtf : <http://recherche.ircam.fr/equipes/salles/listen/download.html>.
12. MIT Kemar Hrtf : <http://sound.media.mit.edu/resources/KEMAR.html>.
13. Floyd E. Toole, *Sound Reproduction*, Elsevier, ISBN 978-0-240-520094, 2004.



The author may be reached at: [manu.degeest@lmsintl.com](mailto:manu.degeest@lmsintl.com).